ADVANCES IN ATMOSPHERIC SCIENCES, VOL. 31, SEPTEMBER 2014, 1147–1156

Simulation and Causes of Eastern Antarctica Surface Cooling Related to Ozone Depletion during Austral Summer in FGOALS-s2

YANG Jing*[1], BAO Qing[2], JI Duoying[3], GONG Daoyi[1], MAO Rui[1], ZHANG Ziyin[4], and Seong-Joong KIM[5]

[1]*State Key Laboratory of Earth Surface Processes and Resource Ecology, Beijing Normal University, Beijing* 100875

[2]*State Key Laboratory of Numerical Modeling for Atmospheric Sciences and Geophysical Fluid Dynamics, Institute of Atmospheric Physics, Chinese Academy of Sciences, Beijing* 100029

[3]*College of Global Change and Earth System Science, Beijing Normal University, Beijing* 100875

[4]*Beijing Meteorological Bureau, Beijing* 100089

[5]*Korea Polar Research Institute, Incheon* 406-130*, Korea*

(Received 5 July 2013; revised 25 December 2013; accepted 6 January 2014)

ABSTRACT

Two parallel sets of numerical experiments (an ozone-hole simulation and a non-ozone-hole simulation) were performed to investigate the effect of ozone depletion on surface temperature change using the second spectral version of the Flexible Global Ocean–Atmosphere–Land System model (FGOALS-s2), focusing on the eastern Antarctica (EA) continent in austral summer. First, we evaluated the ability of the model to simulate the EA surface cooling, and found the model can successfully reproduce the cooling trend of the EA surface, as well as the circulation change circling the South Pole in the past 30 years. Second, we compared the two experiments and discovered that the ozone depletion causes the cooling trend and strengthens the circumpolar westerly flow. We further investigated the causes of the EA surface cooling associated with the ozone hole and found two major contributors. The first is the ozone-hole direct radiation effect (DRE) upon the surface that happens because the decrease of the downward longwave (LW) radiation overcomes the increase of the downward shortwave (SW) radiation under clear sky. The second is the cloud radiation effect (CRE) induced by ozone depletion, which happens because the decreased downward SW radiation overcomes the increased downward LW radiation in the case of increased cloud. Although the CRE is theoretically opposite to the DRE, their final net effect makes comparable contributions to the EA surface cooling. Compared with the surface radiation budget, the surface heat flux budgets have a much smaller contribution. We additionally note that the CRE is basically ascribed to the circulation change.

Key words: ozone depletion, eastern Antarctica surface cooling, numerical simulation

Citation: Yang, J., Q. Bao, D. Y. Ji, D. Y. Gong, R. Mao, Z. Y. Zhang, and S.-J. Kim, 2014: Simulation and causes of eastern Antarctica surface cooling related to ozone depletion during austral summer in FGOALS-s2. *Adv. Atmos. Sci.*, **31**(5), 1147–1156, doi: 10.1007/s00376-014-3144-1.

1. Introduction

In contrast to global warming, the high plateau and coastal regions of eastern Antarctica (EA) show a marked cooling trend, particularly during austral summer, from the 1970s to the early 2000s (e.g., Thompson and Solomon, 2002; Monaghan et al., 2008; Screen and Simmonds, 2012). The cooling trend over the EA surface through the early 2000s has been found to be consistent with the observed trend toward a high index polarity of the Southern Annular Mode (SAM) (e.g., Monaghan et al., 2008; Marshall et al., 2011), which has a close linkage with the Antarctic ozone hole (e.g., Gillett and Thompson, 2003; Fogt et al., 2009; Thompson et al., 2011).

We have confidence in the linkage between the ozone depletion and surface-cooling trend over EA (Thompson et al., 2011), but we do not yet fully understand how the stratospheric ozone depletion causes the EA surface cooling. The stratospheric ozone depletion has two major effects on the troposphere and surface. The first is a radiative effect involving two contrasting processes: increased ultraviolet and visible radiation reaching the surface (e.g., Ramanathan and Dickinson, 1979), but reduced downward thermal infrared radiation to the surface (e.g., Grise and Thompson, 2009), both of which determine the net adjusted radiative forcing reaching the surface. Is the net surface radiative forcing associated with the ozone hole negative or positive? The answer is uncertain (e.g., Hu et al., 2011; Previdi and Polvani, 2012). The radiative forcing could be positive because the shortwave

* Corresponding author: YANG Jing
Email: yangjing@bnu.edu.cn

(SW) forcing dominates the thermal infrared forcing, but the cooling stratosphere might reduce the downward infrared radiation enough to make the net adjusted radiative forcing negative (e.g., Lal et al., 1987; Forster and Shine, 1997). Additionally, clouds could modify the net radiative forcing of the ozone hole reaching the surface. It is well known that clouds reflect shortwave radiation but increase downward longwave (LW) radiation, which counteracts the ozone-hole-related direct radiation forcing. In addition, Ramanathan and Dickinson (1979) found that 50% of downward infrared radiation from stratospheric ozone is absorbed by tropospheric high clouds, such that clouds again decrease the downward LW radiation in this sense. Therefore, cloud-amount change, which could be influenced by ozone depletion, further increases the uncertainties of net radiation forcing reaching the surface.

The other effect is a dynamical one, associated with circulation variation induced by ozone depletion. Related to ozone depletion, the most significant circulation variation is the enhanced circumpolar westerly jet (e.g., Gillett and Thompson, 2003). On the one hand, this strengthened westerly jet tends to isolate most of Antarctica and leads to a reduction in meridional advection of heat onto the continent, cooling the polar region (e.g., Thompsonet al., 2000; Barnes and Hartmann, 2010); but on the other hand, the intensified westerly winds reduce the blocking effect of the Antarctic Peninsula, leading to a higher frequency of relatively warm air masses being advected eastward over the orographic barrier of the northern peninsula (Marshall et al., 2006). Therefore, how the ozone-hole-associated circulation change contributes to the surface cooling has yet to be clarified.

Due to the paucity of data over Antarctica, it is hard to quantify the effect of radiation (including clouds) and circulation from an observational perspective. Numerical model outputs have been considered to be a reasonable method to differentiate the contribution of the above-mentioned effects (radiation, cloud, and circulation) to surface temperature change (e.g., Qu et al., 2012). In addition, numerical experiments are able to specify the effect of ozone depletion through sensitivity experiments. Most previous numerical research has studied the effect of ozone depletion on circulation or temperature through IPCC Fourth Assessment Report (AR4) multi-model outputs (e.g., Cordero and Forster, 2006; Hu et al., 2011; Qu et al., 2012), atmosphere-only model experiments (e.g., Polvani et al., 2011), or radiation–convection models (e.g., Lal et al., 1987; Wang et al., 1993), but seldom via quantitative studies of the contributions of ozone-hole-induced radiation or circulation to surface temperature change.

FGOALS-s2 (the second spectral version of the Flexible Global Ocean–Atmosphere–Land System model) is a newly released coupled general circulation model that participated in IPCC AR5 (Fifth Assessment Report). Through two sets of numerical experiments, this study first evaluates the performance of the EA surface cooling in this model, and then investigates the relative quantitative contributions of radiation and circulation associated with ozone depletion to the EA surface cooling.

2. Model and numerical experiments

2.1. *Model*

The climate system model used in this study is FGOALS-s2, which can provide realistic climate simulations (Bao et al., 2013). The atmospheric component is SAMIL–the Spectral Atmospheric Model of the Institute of Atmospheric Physics (IAP)/State Key Laboratory of Numerical Modeling for Atmospheric Sciences and Geophysical Fluid Dynamics (LASG) (Bao et al., 2010), and its horizontal resolution is 2.81° (lon) ×1.66° (lat), with 26 hybrid vertical layers. The oceanic component is the LASG IAP Common Ocean Model 2.0 (LICOM2.0) (Liu et al., 2012). Compared with the old version of LICOM (Liu et al., 2004), the horizontal resolution in LICOM2.0 was increased in the tropics (from $1^\circ \times 1^\circ$ to $0.5^\circ \times 0.5^\circ$), and the vertical resolution was adjusted to 10-m layer thicknesses in the upper 150 m (Liu et al., 2012). In addition, a new advection scheme and mixing schemes were introduced and updated in LICOM2.0. The sea ice model in FGOALS-s2 is version five of the Community Sea Ice Model (CSIM5), which is a thermodynamic–dynamic sea ice model (Briegleb et al., 2004). The other components, including the land surface and coupler components, are similar to those in version four of the National Center for Atmospheric Research (NCAR) Community Climate System Model (CCSM4) (Kiehl and Gent, 2004).

2.2. *Numerical design and methodology*

In order to determine the response of Antarctic surface climate to ozone depletion, two sets of numerical experiments were performed. One was a control run (also called "ozone-hole-run", or the "OH run" for short), which was a standard run based on the CMIP5 (Coupled Model Intercomparison Project, Phase 5) experimental design (Taylor et al., 2012), and was integrated from 1850 to 2005. The imposed changing conditions in the OH run included atmospheric composition (including O_3 and CO_2) due to anthropogenic and volcanic influences, solar forcing, concentrations of short-lived species, and aerosols. Therefore, the OH run involved the realistic ozone depletion that has taken place since the 1970s (Solomon, 1999; WMO, 2007). The other experiment was the ozone sensitivity run (also called "no-ozone-hole run", or the "NOH run" for short), which was performed with the same configuration as CMIP5 historical runs from 1850 to 2005, but the forcing of ozone after 1976 was left at 1975 levels because the severe depletion of Antarctica stratospheric ozone occurred from the late 1970s onwards (Solomon, 1999). In order to reduce the uncertainties arising from differing initial conditions, both the OH and NOH runs had three individual ensemble members, each starting from different initial conditions derived from the pre-industrial experiment. The results of each simulation were derived from the three-ensemble mean during the 30 years from 1976 to 2005, and the impact of ozone depletion on Antarctica surface temperature is diagnosed in this paper by comparing the two sets of 30-yr simulations during that period.

We used the Student's *t*-test for the linearized trend sig-

nificance, and a Monte Carlo simulation to establish the confidence level of the tendency difference between the two experiments (OH minus NOH). In terms of the detail of the Monte Carlo simulation, first we re-sampled the OH time series 1000 times in order to obtain 1000 tendency differences against the NOH time series. Then, we calculated the PDF (probability density function) for those 1000 tendency differences. If the tendency difference obtained was located in the $< 10\%$ region, we were able to conclude that the tendency difference was above the 90% confidence level.

2.3. *Ozone forcing data*

The ozone forcing dataset used in this study was from the Atmospheric Chemistry and Climate and the Stratosphere–Troposphere Processes and their Role in Climate (SPARC) committees of the World Climate Research Program (WCRP) (Randel and Wu, 2007). This study concerns the differences before and after the formation of the ozone hole. So, the physical extent of the ozone hole is at the basis of our work. Figure 1 demonstrates the seasonal, latitudinal and vertical characteristics of the ozone hole during 1976–2005, according to SPARC data. Three features are particularly noteworthy. First, the Southern Hemisphere ozone hole peaks in October, and the depletion lasts from September to November. Second, the latitudinal extent of the ozone hole spans nearly 30° of latitude, from the South Pole to 60°S. And third, the stratospheric ozone hole peaks at 50 hPa. Since the ozone hole leads the cooling response of the polar region by one to two months, and the surface cooling trend over EA is most significant during austral summer (Randel and Wu, 2007; Ramaswamy et al., 2001; Thompson and Solomon, 2002), this study focuses on the austral summer season (December–January–Feburary, DJF).

3. Simulation of eastern Antarctica surface cooling associated with ozone depletion

The surface cooling over EA has been observed in long-term station data (e.g., Thompson and Solomon, 2002). To evaluate the simulation of the EA surface cooling in the model, we first calculated the surface temperature trend in past 30 years from 1976 to 2005 using three types of datasets: Antarctica station data (http://www.antarctica.ac.uk/met/); Delaware land surface data (http://jisao.washington.edu/data_sets/ud/); and ERA-interim surface reanalysis data (Dee et al., 2011); the results of which are shown in Fig 2. We can see that the coastal EA station shows an evident cooling trend by $-0.5\ ^\circ$ (10 yr)$^{-1}$ to -1.5° (10 yr)$^{-1}$. Furthermore, almost the same cooling amplitude can be seen in the Delaware data and the ERA-interim reanalysis data. With the forcing of realistic ozone depletion, the surface cooling trend over the EA surface is captured in the model's OH run but has a smaller magnitude of only 0 to -0.5° (10 yr)$^{-1}$ (Fig. 3a).

In contrast, the cooling trend disappears in the NOH run (Fig. 3b). Therefore, the simulated cooling trend is induced by ozone depletion, which is consistent with several previous studies (e.g., Thompson et al., 2011). To quantify the contribution of ozone depletion to the EA surface cooling, we calculated the difference between the two experiments (OH–NOH), and the results show that the ozone hole causes the largest surface cooling amplitude over the EA continent, and the maximum magnitude reaches -0.7° (10 yr)$^{-1}$ in the simulation (Fig. 3c).

A strengthening of the westerly flow throughout the troposphere at around 60°–70°S is reproduced in the OH run, which is consistent with many observational studies (e.g., Shindell and Schmidt, 2004) (Figs. 4a and b). Comparing

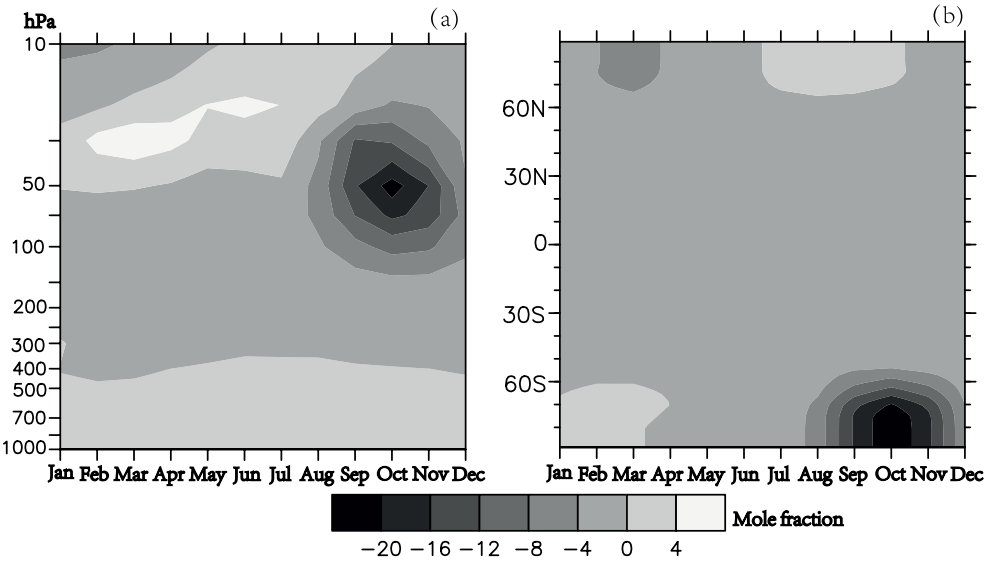

Fig. 1. The horizontal and vertical extents of the ozone hole (difference between climatology of 1976–2005 and 1975) used in this study based on the SPARC ozone datasets: (a) vertical extent over the polar cap averaged over the area south of 65°S by month; (b) zonal mean latitudinal cross section at 50 hPa by month.

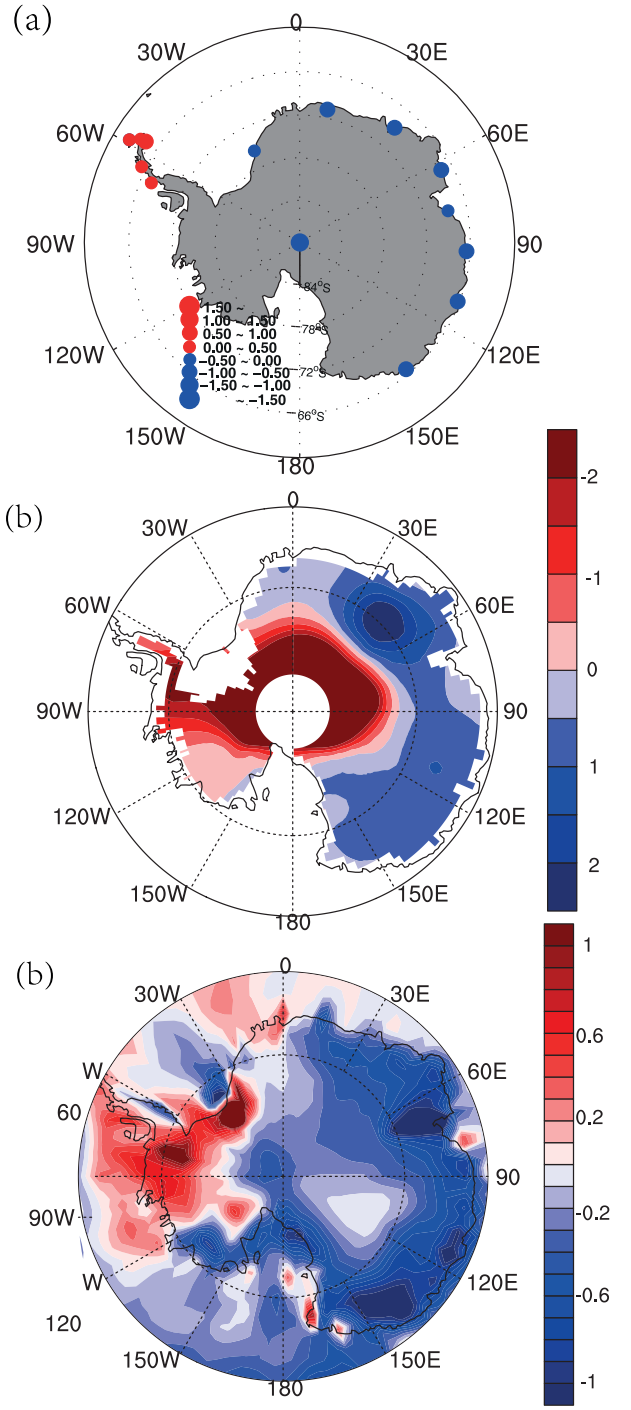

Fig. 2. Austral summer surface temperature trends [K (10 yr)$^{-1}$] from 1976 to 2005 retrieved from (a) Antarctica station data, (b) Delaware land data, and (c) ERA-interim reanalysis data.

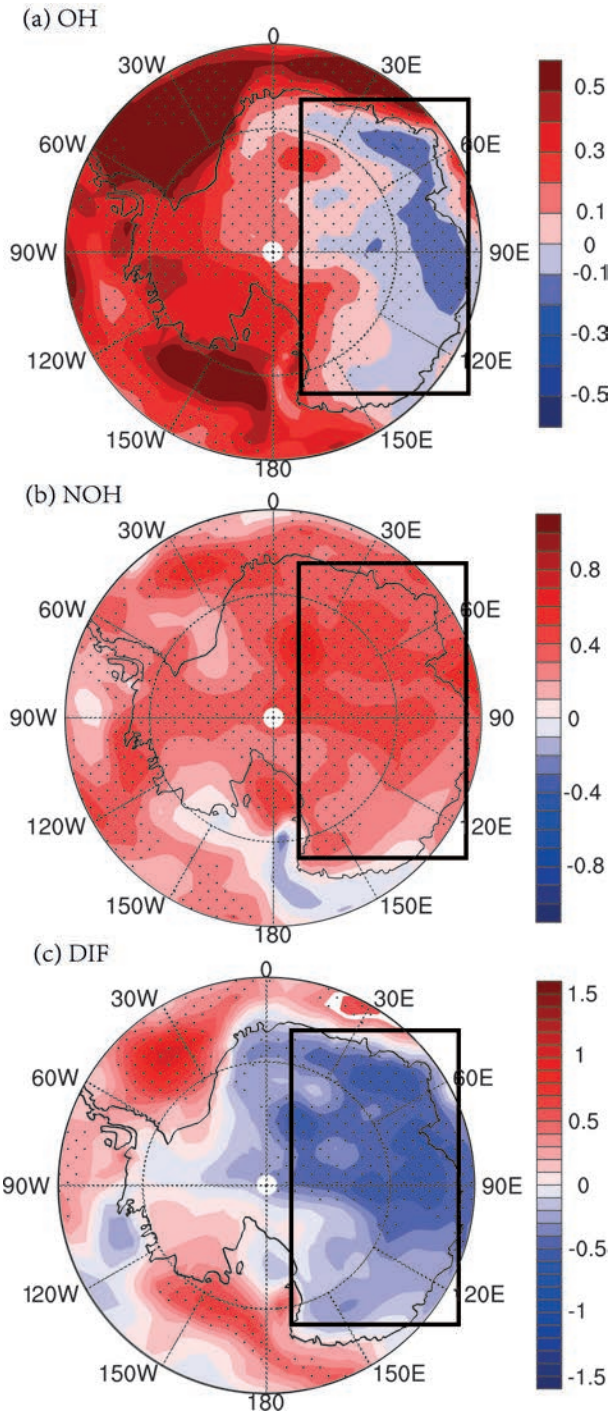

Fig. 3. Austral summer surface temperature trends [K (10 yr)$^{-1}$] from 1976 to 2005 for the (a) OH results, (b) NOH results, and (c) their difference (OH minus NOH). Dotted regions are above the 90% confidence level according to the Student's *t*-test.

the two experiments, the ozone depletion evidently strengthens the westerly flow encircling the polar cap (Fig. 4c) due to an increased north-south temperature gradient (Fig. 5).

The above evaluations indicate that this model is able to reproduce the austral summer surface-cooling trend over EA in the past three decades. Meanwhile, the circulation change and its responses to ozone depletion in the simulation are reasonable according to previous studies.

4. Causes of the eastern Antarctica surface cooling related to ozone depletion in the simulation

In order to investigate how the ozone depletion causes the EA surface cooling in this numerical study, we analyze

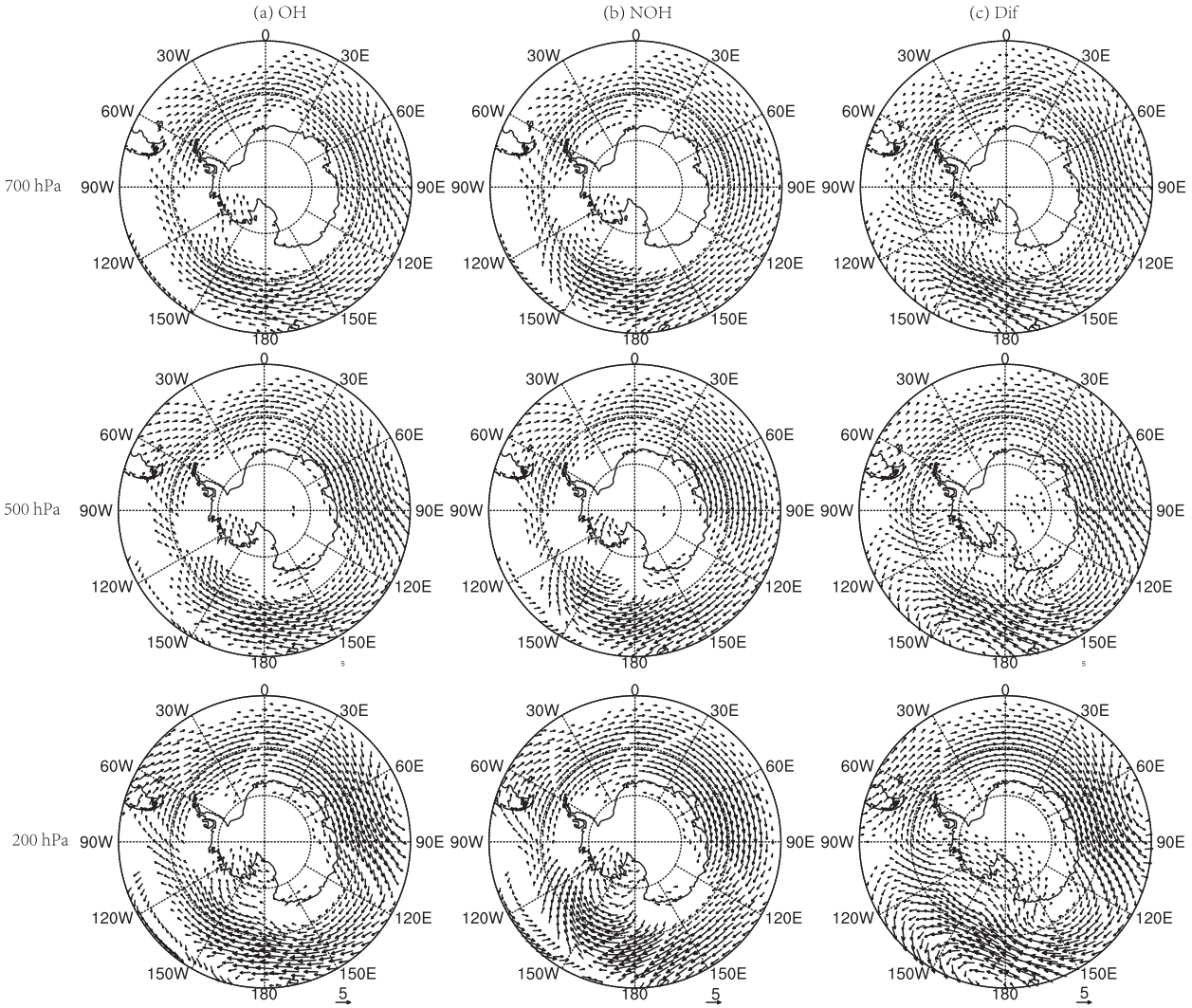

Fig. 4. Linearized trend of 700 hPa (upper row), 500 hPa (middle row), and 200 hPa (lower row) winds [m s^{-1} (10 yr)$^{-1}$] for the (a) OH run, (b) NOH run, and (c) their difference. Vectors are shown above the 90% confidence level.

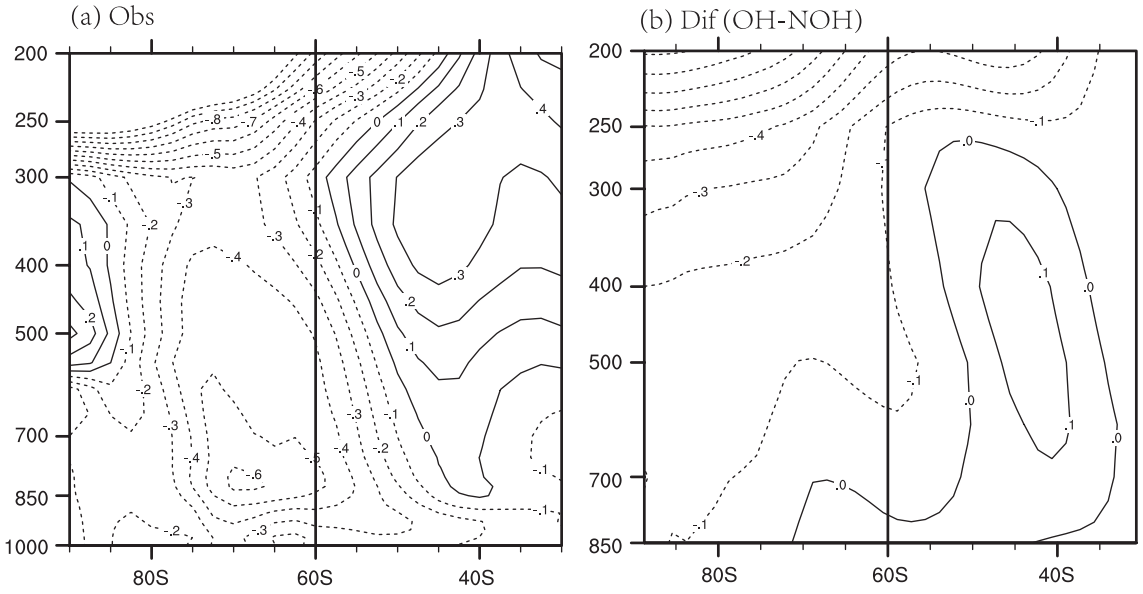

Fig. 5. Zonal mean austral summer temperature trend [K (10 yr)$^{-1}$] along with height (units: hPa) in (a) observation (ERA-interim) and (b) difference between the OH and NOH model runs.

the direct radiation effect (DRE) under clear sky, the cloud radiation effect (CRE) and the possible dynamical effect associated with the ozone hole on the surface, measured by the trend differences between the two experiments (OH minus NOH). All variables we discuss below are the differences between the two experiments.

We first calculated the ozone-hole-induced DRE down upon the surface without considering cloud, respectively including downward LW radiation and downward SW radiation under clear sky. The results show that, over EA, and accompanied by ozone depletion, downward LW radiation has a negative trend and downward SW radiation has a positive trend (Figs. 6a and b); this is because ozone can physically absorb the ultraviolet radiation (e.g., Ramanathan and Dickinson, 1979) and emit the downward thermal infrared radiation to the surface (e.g., Grise and Thompson, 2009). The magnitude of the decreased LW radiation is around -1 to -2 W m^{-2} (10 yr)$^{-1}$, and the increased SW radiation is around -0.5 to -1 W m^{-2} (10 yr)$^{-1}$ (Figs. 6a and b). Consequently, the net downward DRE is negative at -0.5 to -1 W m^{-2} (10 yr)$^{-1}$ (Fig. 6c). In this case, the decrease of downward LW radiation overcoming the increase of downward SW radiation becomes one of the principle contributors to the surface cooling under clear sky when ozone depletion occurs.

Cloud is an important factor influencing the downward radiation reaching the surface. For example, increased cloud cover blocks downward SW radiation and increases downward LW radiation, which is theoretically the opposite to the DRE of ozone depletion. But what about the net CRE in this numerical study? We first calculated the cloud change associated with ozone depletion from two aspects: cloud fraction, and cloud liquid content (cloud liquid content determines cloud optical depth), which are two decisive factors of CRE (Wood et al., 2007). From the results we can see that the cloud fraction (here, the cloud cover mainly includes high cloud because the EA continent is cold and at high altitudes) mainly exhibits an increasing trend over EA, especially over the eastern part (Fig. 7a). The region with increased cloud fraction generally features increased mass fraction of cloud liquid content (calculated as the mass of cloud liquid water in the grid cell divided by the mass of air including the water in all phases in the grid cells) and the most evident increase of cloud liquid water fraction occurs over the eastern part of EA (Fig. 7b).

To quantify the corresponding CRE, we calculated the differences between clear-sky and cloudy-sky downward LW, downward SW, and downward net radiation. As shown in Figs. 8a and b, the region with increased cloud cover generally corresponds to increased downward LW radiation and decreased downward SW radiation. It is interesting that the net CRE is negative over EA (Fig. 8c), with a magnitude of -0.5 to -1 W m^{-2} (10 yr)$^{-1}$, because the decreased downward SW radiation overcomes the increased downward LW radiation in amplitude. The reasons for the relatively small amplitude of increased LW radiation are related to the two opposite cloud effects on LW radiation: clouds emit downward LW radiation as well as absorb downward LW radiation from stratospheric ozone (Ramanathan and Dickinson, 1979). Therefore, although CRE and DRE are almost contracting with each other in theory, as mentioned above, their net effects both result in comparable cooling in the model results.

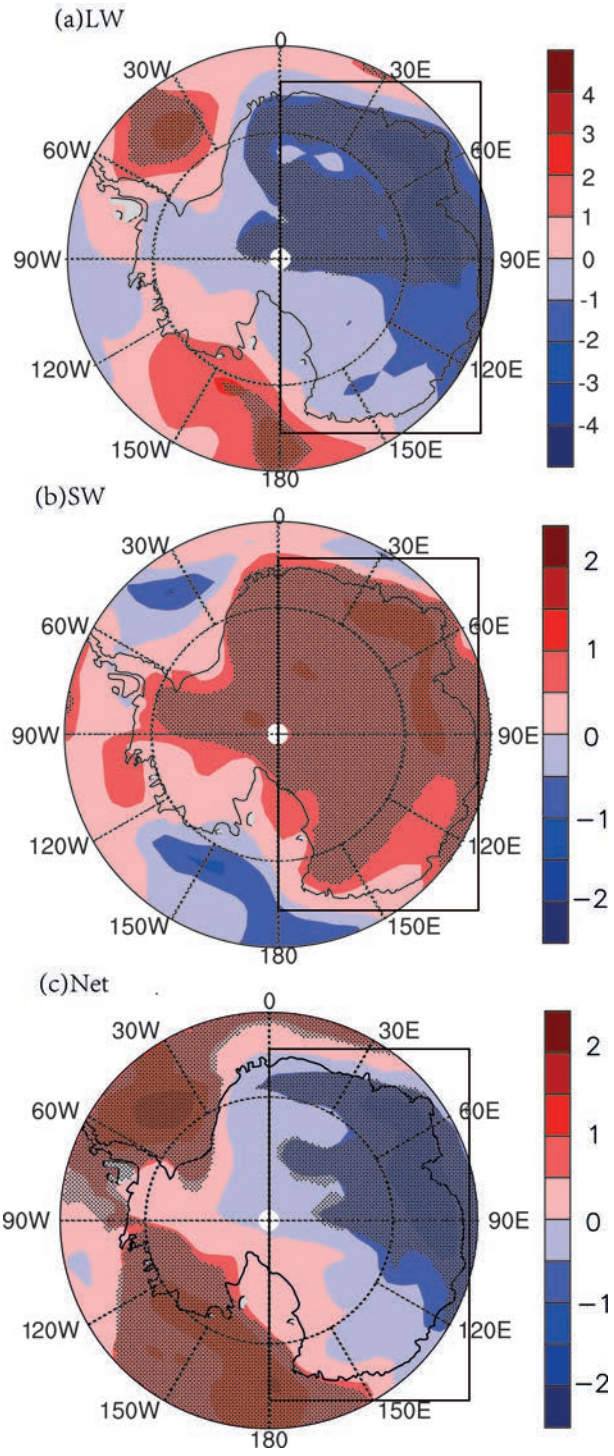

Fig. 6. Austral summer tendency differences of surface downward ozone-associated direct radiation fluxes (under clear sky) for (a) LW, (b) SW, and (c) net downward radiation (LW+SW) from 1976 to 2005 [units: W m^{-2} (10 yr)$^{-1}$]. Dotted regions are above the 90% confidence level.

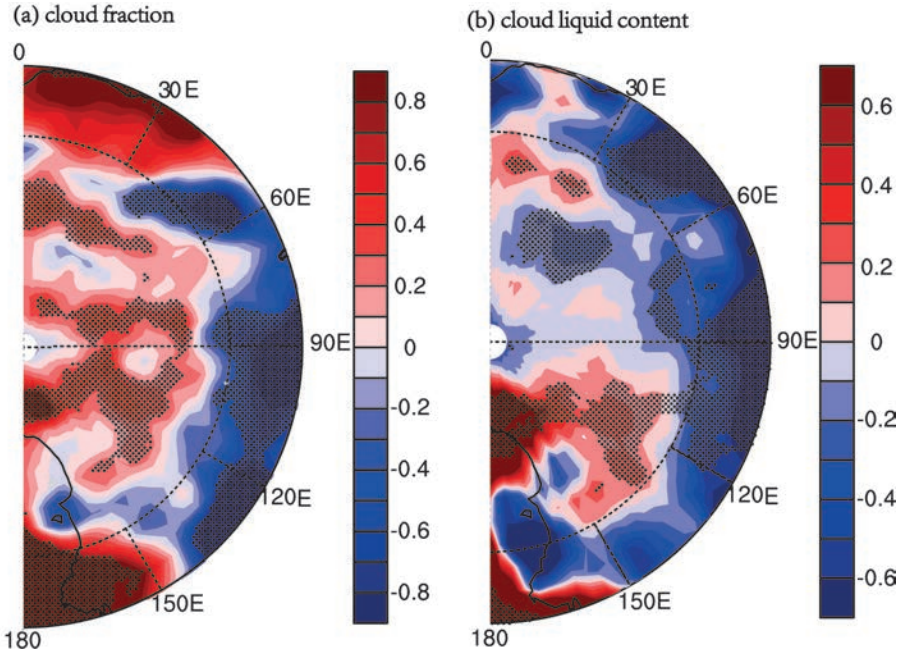

Fig. 7. Austral summer tendency differences of cloud fraction and cloud liquid water mass fraction (calculated as the mass of cloud liquid water in the grid cell divided by the mass of air including the water in all phases in the grid cells) from 1976 to 2005 (units: 100%). Dotted regions are above the 90% confidence level.

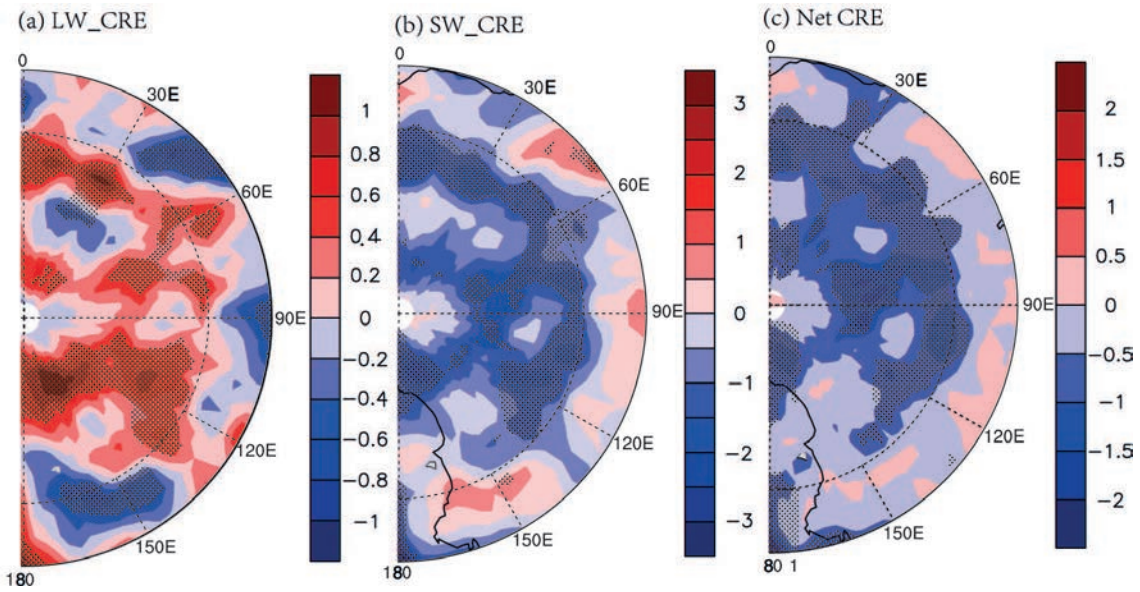

Fig. 8. Austral summer tendency differences of surface downward radiation fluxes caused by the CRE for (a) LW, (b) SW, and (c) net downward radiation (LW+SW) from 1976 to 2005 [units: W m^{-2} (10 $yr)^{-1}$]. Dotted regions are above the 90% confidence level.

Hence, the increased cloud associated with ozone depletion is another principle contributor to the EA surface cooling.

The next question is why the cloud fraction has an increasing trend with ozone depletion, particularly over the eastern portion of EA. To address this, we investigated the vertical velocity change and found that the eastern portion of EA is characterized by an ascending trend (Fig. 9a), which causes the increase of the cloud fraction. The increased ascending trend could possibly be ascribed to the increase of westerly flow and the formation of the local cyclonic anomaly (Fig. 9b). Additionally, there is also a possibility that the increased upward motion could be enhanced by the orographic lift over EA. Thus, the CRE on cooling basically results from dynamical circulation change.

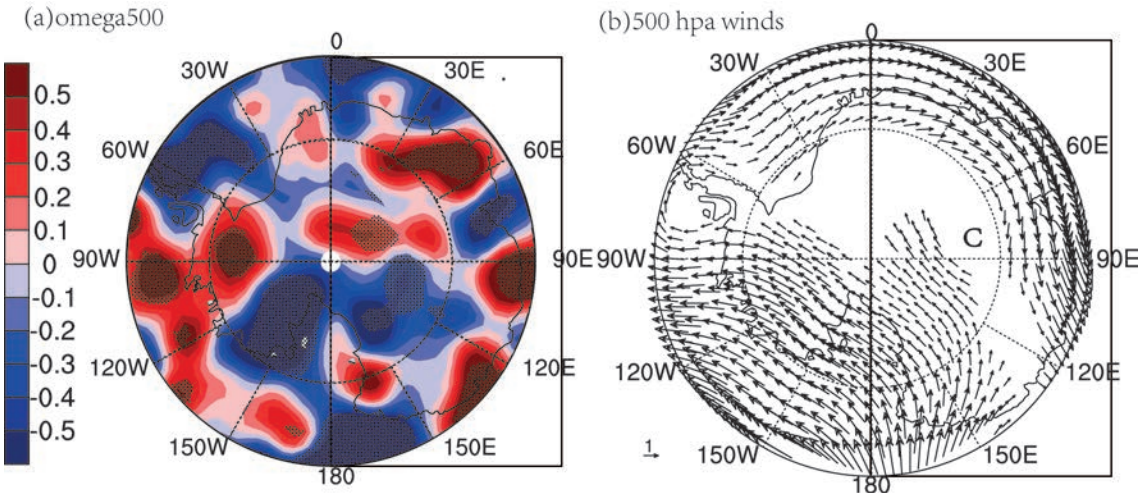

Fig. 9. Austral summer tendency differences of 500 hPa vertical velocity (down is positive) and 500 hPa winds [units: m s^{-1} (10 yr)$^{-1}$]. Dotted regions are above the 90% confidence level, and vectors shown are above the 90% confidence level.

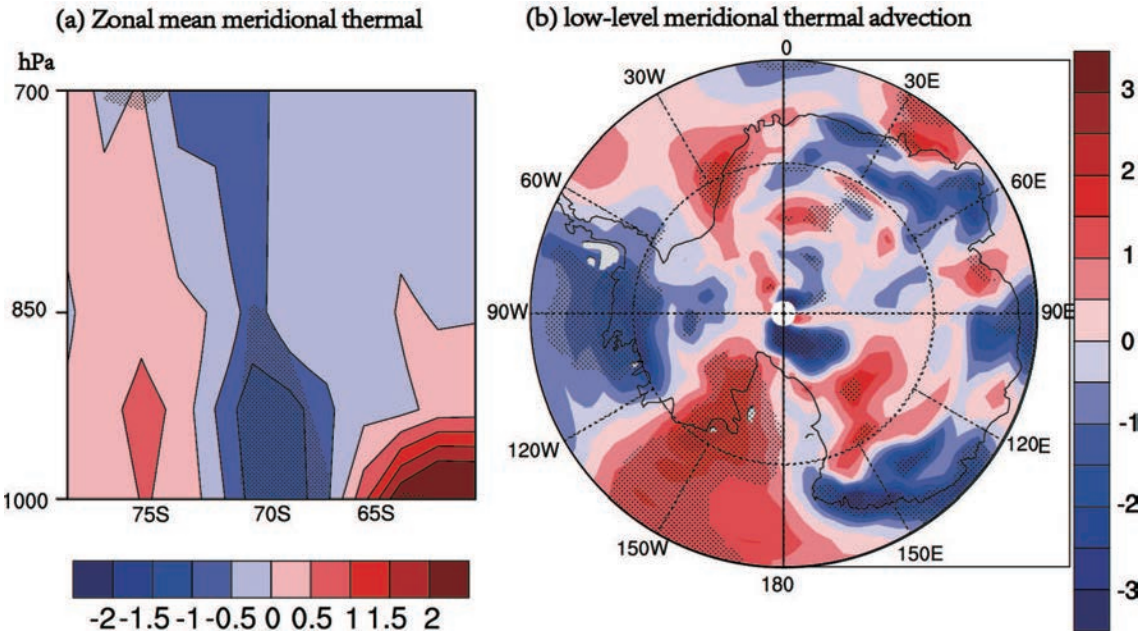

Fig. 10. (a) Zonal mean meridional thermal advection below 700 hPa; (b) low-level meridional thermal advection trend between 1000 hPa and 700 hPa. All the above are the austral summer tendency differences between the two experiments (OH minus NOH). Units are K s^{-1} (10 yr)$^{-1}$. Dotted regions are above the 90% confidence level.

In addition to the above two radiation effects, we also calculated the changes in surface sensible heating (SH) and surface latent heating (LH) fluxes (figures omitted). The results show that the magnitude of the LH trend is much smaller [below 0.05 W m^{-2} (10 yr)$^{-1}$], which can be ignored in the analysis. The upward SH flux trend is positive, but smaller [0.1–0.3 W m^{-2} (10 yr)$^{-1}$] than the radiation effect [the amount of ozone-direct radiation plus the CRE is around −1.0 to −2.0 W m^{-2} (10 yr)$^{-1}$].

Previous studies have pointed out that a strengthened westerly jet can cause a reduction in meridional advection of heat onto the Antarctica continent (e.g., Thompson et al., 2000; Barnes and Hartmann, 2010). Our result does indeed show that the ozone depletion causes a significant negative trend of the total heat advection averaged around 70°S in the lower troposphere (Fig. 10a). However, when we examine the low-level spatial distribution of thermal advection over the EA cooling region (Fig. 10b), we find that half of the EA region features warming advection trends. This result hints that the lower-level thermal advection is not an obvious cause for the EA surface cooling, at least as revealed by the results of this numerical study.

5. Concluding remarks

In this study, we first evaluated the ability of FGOALS-s2 to simulate the surface climate change over the Antarctic, and found that the OH run (control) of FGOALS-s2 was able to reproduce the surface-cooling trend over the EA continent and strengthened circumpolar westerly flow in the past 30 years; however, the EA cooling amplitude was smaller than observed. Without the ozone hole, both the surface cooling and the intensified circumpolar westerly were remarkably weakened in the NOH simulation. Therefore, the effects of ozone depletion on enhancing the surface cooling and strengthening the westerly stream in the simulation were consistent with many previous studies.

Comparing the two numerical experiments, we further analyzed the surface budget change to investigate the causes of the EA surface cooling and found that the surface radiation change acts as the dominant contributor to the EA cooling which is much larger than the surface heat flux change. The surface radiation changes come from two effects associated with ozone depletion: the DRE (direct radiation effect) and the CRE (cloud radiation effect). The DRE and CRE cause comparable surface cooling over EA although they have opposite effects when accompanied by ozone depletion. The DRE causes cooling because the decrease of downward LW radiation is larger than the increase of downward SW radiation, and the CRE causes cooling because the decreased downward SW radiation is larger than the increased downward LW radiation. In the final analysis, the CRE was actually found to be associated with a dynamical circulation effect. In this sense, the radiation effect and dynamical effect play comparable roles in the causes of surface cooling over EA.

Acknowledgements. This study was supported by the project "Investigation of Climate Change Mechanisms by Observation and Simulation of the Polar Climate Past and Present" (PE14010) of the Korea Polar Research Institute, the National Natural Science Foundation of China (Grant No. 41375003), the Beijing High Education Young Elite Teacher Project and the Chinese Academy of Sciences (Grant No. XDA05110303).

REFERENCES

Bao, Q., G. X. Wu, Y. M. Liu, J. Yang, Z. Z. Wang, and T. J. Zhou, 2010: An introduction to the coupled model FGOALS1.1-s and its performance in East Asia. *Adv. Atmos. Sci.*, **27**, 1131–1142. doi: 10.1007/s00376-010-9177-1.

Bao, Q., and Coauthors, 2013: The flexible global ocean-atmosphere-land system model, spectral version 2: FGOALS-s2. *Adv. Atmos. Sci.*, **30**, 561–576, doi: 10.1007/s00376-012-2113-9.

Barnes, E. A., and D. L. Hartmann, 2010: Dynamical feedbacks of the southern annular mode in winter and summer. *J. Atmos. Sci.*, **67**, 2320–2330.

Briegleb, B. P., C. M. Bitz, E. C. Hunke, W. H. Lipscomb, M. M. Holland, J. L. Schramm, and R. E. Moritz, 2004: Scientific description of the sea ice component in the community climate system model. 3rd version. NCAR Tech. Note, 70 pp.

Cordero, E. C., and P. M. Forster, 2006: Stratospheric variability and trends in models used for the IPCC AR4. *Atmos. Chem. Phys.*, **6**, 5369–5380.

Dee, D. P., and Coauthors, 2011: The ERA-Interim reanalysis: Configuration and performance of the data assimilation system. *Quart. J. Roy. Meteor. Soc.*, **137** 553–597.

Fogt, R. L., J. Perlwitz, and A. J. Monaghan, 2009: Historical SAM variability. Part II: Twentieth-century variability and trends from reconstructions, observations, and the IPCC AR4 Models. *J. Climate*, **22**, 5346–5365.

Forster, P. M. D., and K. P. Shine, 1997: Radiative forcing and temperature trends from stratospheric ozone changes. *J. Geophys. Res.*, **102**, 10 841–10 855.

Gillett, N. P., and D. W. J. Thompson, 2003: Simulation of recent Southern hemisphere climate change. *Science*, **302**, 273–275.

Grise, K. M., and D. W. J. Thompson, 2009: On the role of radiative processes in stratosphere-troposphere coupling. *J. Climate*, **22**, 4154–4161.

Hu, Y., Y. Xia, and X. Fu, 2011: Tropospheric temperature response to stratospheric ozone recovery in the 21st century. *Atmos. Chem. Phy.*, **11**, 7687–7699.

Kiehl, J. T., and P. R. Gent, 2004: The community climate system model, version 2. *J. Climate*, **17**, 3666–3682.

Lal, M., A. K. Jain, and M. C. Sinha, 1987: Possible climatic implications of depletion of Antarctic ozone. *Tellus*, **38**, 326–328.

Liu, H. L., Y. Q. Yu, W. Li, and X. H. Zhang, 2004: *Manual for LASG/IAP Climate System Ocean Model* (*LICOM1. 0*). Science Press, Beijing, 128 pp. (in Chinese)

Liu, H. L., P. F. Lin, Y. Q. Yu, and X. H. Zhang, 2012: The baseline evaluation of LASG/IAP climate system ocean model (LICOM) version 2. *Acta Meteorologica Sinica*, **26**, 318–329, doi: 10.1007/s13351-012-0305-y.

Marshall G. J., A. Orr, N. P. M. van Lipzig, and J. C. King, 2006: The impact of a changing Southern Hemisphere annular mode on Antarctic Peninsula summer temperatures. *J. Climate*, **19**, 5388–5404.

Marshall, G. J., D. B. Stefano, and S. S. Naik, 2011: Analysis of a regional change in the sign of the SAM-temperature relationship in Antarctica. *Climate Dyn.*, **36**, 277–287.

Monaghan, A. J., D. H. Bromwich, H. David, and W. Chapman, 2008: Recent variability and trends of Antarctic near-surface temperature. *J. Geophys. Res.*, **113**, D04105, doi: 10.1029/2007JD009094.

Polvani, L. M., W. W. Darryn, J. P. Gustavo, and S. W. Son, 2011: Stratospheric ozone depletion: The main driver of twentieth-century atmospheric circulation changes in the Southern Hemisphere. *J. Climate*, **24**, 795–812.

Previdi, M., and L. M. Polvani, 2011: Comment on "Tropospheric temperature response to stratospheric ozone recovery in the 21st century" by Hu et al. (2011). *Atmos. Chem. Phys.*, **12**, 4893–4896.

Qu, X., A. Hall, and B. Julien, 2012: Why does the Antarctic Peninsula warm in climate simulations? *Climate Dyn.*, **38**, 913–927.

Ramanathan, V., and R. E. Dickinson, 1979: The role of stratospheric ozone in the zonal and seasonal radiative energy balance of the earth-troposphere system. *J. Atmos. Sci.*, **36**, 1084–1104.

Ramaswamy, V., and Coauthors, 2001: Stratospheric temperature trends: Observations and model simulations. *Rev. Geophys.*,

39, 71–122, doi: 10.1029/1999RG000065.

Randel, W. J., and F. Wu, 2007: A stratospheric ozone profile data set for 1979–2005: Variability, trend and comparison with column ozone data. *J. Geophys. Res.*, **112**, D06313 doi: 10.1029/2006JD007339.

Screen, J. A., and I. Simmonds, 2012: Half-century air temperature change above Antarctica: Observed trends and spatial reconstructions. *J. Geophys. Res.*, D16108, doi: 10.1029/2012JD 017885.

Shindell, D. T., and G. A. Schmidt, 2004: Southern Hemisphere climate response to ozone changes and greenhouse gas increases. *Geophys. Res. Lett.*, **31**, L18209, doi: 10.1029/2004 GL020724.

Solomon, S., 1999: Stratospheric ozone depletion: A review of concepts and history. *Rev. Geophys.*, **37**, 275–316. doi: 10.1029/1999RG900008.

Taylor, K. E., R. J. Stouffer, and G. A. Meehl, 2012: An overview of CMIP5 and the experiment design. *Bull. Amer. Meteor. Soc.*, **93**, 485–498.

Thompson, D. W. J., and S. Solomon, 2002: Interpretation of recent Southern Hemisphere climate change. *Science*, **296**, 895–899.

Thompson, D. W. J., J. M. Wallace, and G. C. Hegerl, 2000: Annular modes in the extratropical circulation. Part II: Trends. *J. Climate*, **13**, 1018–1036.

Thompson, D. W. J., S. Solomon, P. J. Kushner, M. H. England, K. M. Grise, and D. J. Karoly, 2011: Signatures of the Antarctic ozone hole in Southern Hemisphere surface climate change. *Nature Geoscience*, **4**, 741–749.

Wang, W.-C., Y. C. Zhuang, and R. D. Uojkov, 1993: Climate implications of observed changes in ozone vertical distributions at middle and high latitudes of the northern hemisphere *Geophys. Res. Lett.*, **20**, 1567–1570, doi: 10.1029/93GL01318.

World Meteorological Organization (WMO), 2007: Scientific assessment of ozone depletion, 2006. WMO Global Ozone Research and Monitoring Project Rep. No. 50, Geneva, 572 pp.

Wood, R, B. Huebert, C. R. Mechoso, and R. Weller, 2007: The VAMOS Ocean-Cloud-Atmosphere-Land study. WCRP and Cosponsors Program Summary, 9 pp. [Available online at http://www.eol.ucar.edu/projects/vocals/documentation/vocals_overview.pdf.]